Phenomena in *J*-coupled nuclear magnetic resonance spectroscopy in low magnetic fields

Stephan Appelt,[1,*] F. Wolfgang Häsing,[1] Holger Kühn,[1] and Bernhard Blümich[2]

[1]*Central Institute for Electronics, Research Center Jülich, D-52425 Jülich, Germany*

[2]*Institute for Technical Chemistry and Macromolecular Chemistry, RWTH Aachen, D-52056 Aachen, Germany*

We present the theory and experimental results of phenomena associated to *J*-coupled nuclear magnetic resonance (NMR) spectroscopy at low magnetic fields ($<10^{-4}$ T). So far it was believed that in low field the chemical shift and with it the homonuclear *J*-coupling information is lost. This contribution shows that the network of all homo- and heteronuclear *J*-coupling constants can be measured in low magnetic fields, thus revealing the whole molecular structure even in the absence of any chemical shift information. The chemical group of the form YX_N (Y=rare spin 1/2, X=observed spin 1/2, N=number of spins X) can be identified by the number of lines in the heteronuclear coupled X spectrum if the strong *J*-coupling condition is valid. If two molecular groups, such as YX_N and AX_{M-N} (A=group without nuclear spin, M=total number of coupled spins X), are bound together then all homo- and heteronuclear *J*-coupling constants appear in the X-NMR spectrum as pairs of multiplets. A vector model is presented which explains the relation between the molecular structure and the number of observed lines in a multiplet pair. The linewidths of the different NMR lines inside one multiplet are measured to be substantially different and depend on the total spin state of the molecule. If M is an odd number and $M-1$ spins X of the molecule are coupled into $(M-1)/2$ singlets, then intramolecular dipole-dipole relaxation as well as *J*-coupling mediated relaxation processes are suppressed and very narrow lines are observed.

PACS number(s): 33.25.+k, 32.30.Dx, 82.56.−b, 39.30.+w

I. INTRODUCTION

The chemical shift information [1,2] and the electron mediated indirect nuclear spin-spin interaction [3,4]—the so called *J* coupling—are important NMR parameters for the determination of molecular structures. For NMR in low magnetic fields ($<10^{-4}$ T), for example in the Earth's magnetic field [5–20], the chemical shift information vanishes but the field independent *J*-coupling constants remain. It was believed that in low field the homonuclear *J*-coupling constants are not observable [21,22]. The inductive detection of NMR signals at high magnetic fields are favored over measurements at low field for four reasons: (1) the signal to noise ratio (S/N) increases with increasing magnetic field, (2) chemical shift differences cannot be measured at low magnetic fields, (3) the spectral resolution obtained through well shimmed superconducting high field magnets is better than that from low-field magnets, and (4) the homonuclear *J*-coupling constants appear to be inaccessible for vanishing chemical shift differences.

The development of hyperpolarization and premagnetization techniques [23–31] and of sensitive detection methods [32–38] has made the S/N ratio of NMR signals nearly independent on the magnetic field. This lifts objection (1) against low-field NMR. Referring to objection (2) it was shown that chemical shift differences can be measured even in inhomogeneous low magnetic fields [39,40]. With hyperpolarized ^{129}Xe chemical shifts can be measured with high precision in the Earth's magnetic field [41]. High resolution proton (^{1}H) and fluorine (^{19}F) Earth's field NMR spectroscopy [42] was performed showing the heteronuclear ^{1}H-^{29}Si

and ^{1}H-^{19}F *J*-coupling constants with an accuracy nearly two orders of magnitude better than obtainable by high-resolution NMR at high field, so objection (3) can be dealt with.

In this article we analyze the mathematical framework of *J*-coupled NMR in low magnetic fields, especially in the Earth's magnetic field where the strong *J*-coupling condition is valid with respect to the Larmor frequencies. The strong *J*-coupling regime is entered if the difference in the nuclear Larmor frequencies of two given nuclear species is in the order of the heteronuclear *J*-coupling constant.

II. THEORY

A. General considerations

Why is it impossible in low magnetic fields to measure the homonuclear *J*-coupling constant between pairs of spins in the absence of heteronuclear *J* couplings? Given M spins with angular momentum operator $\vec{I}_k$ ($k=1,\dots,M$) interacting with a magnetic field B_0 applied along the z direction and assuming that all possible spin pairs are homonuclear *J* coupled the Hamilton operator can be written as

$$H = \underbrace{\sum_{k=1}^{M} \omega_{Ik} I_{kz}}_{H_0} + \underbrace{2\pi \sum_{k=1, l=k+1}^{M} J_{Ik,Il}\vec{I}_k \cdot \vec{I}_l}_{H_{\text{hom}}},$$

$$(2.1)$$

where $\omega_{Ik} = \gamma_k(1-\sigma_k)B_0$ is the angular Larmor frequency including the isotropic chemical shift interaction of the spin $\vec{I}_k$, γ_k is the gyromagnetic ratio of spin k, and $J_{Ik,Il}$ denotes the homonuclear *J*-coupling constant between the pair of spins k and l with angular momentum operator $\vec{I}_k$ and $\vec{I}_l$. H_0 and H_{hom} are the Hamilton operators of the Zeeman interaction

*st.appelt@fz-juelich.de

and of all homonuclear *J*-couplings, respectively. After a 90° pulse excitation around the *y* axis one measures the expectation value of the total spin angular momentum $\langle \Sigma_{k=1}^{M} I_{kx} \rangle$. We show that none of the homonuclear *J*-coupling constants $J_{Ik,Il}$ can be measured if we assume that the following two commutator relations

$$\left[\sum_{k=1}^{M} I_{kx}, H_{\text{hom}} \right] = 0 \qquad (2.2)$$

and

$$[H_0, H_{\text{hom}}] = 0 \qquad (2.3)$$

are fulfilled. The evaluation of $\langle \Sigma_{k=1}^{M} I_{kx} \rangle$ by using the time evolution of the initial density matrix $\rho(0) = \Sigma_{k=1}^{M} I_{kx}$ and by applying Eqs. (2.2) and (2.3) results in

$$\left\langle \sum_{k=1}^{M} I_{kx} \right\rangle = \text{Tr} \left\{ \left(\sum_{k=1}^{M} I_{kx} \right) e^{-iHt} \rho(0) e^{iHt} \right\}$$

$$= \text{Tr} \left\{ \left(\sum_{k=1}^{M} I_{kx} \right) e^{-iH_0t} e^{-iH_{\text{hom}}t} \rho(0) e^{iH_0t} e^{iH_{\text{hom}}t} \right\}$$

$$= \text{Tr} \left\{ \left(\sum_{k=1}^{M} I_{kx} \right) e^{-iH_0t} e^{-iH_{\text{hom}}t} \rho(0) e^{iH_{\text{hom}}t} e^{iH_0t} \right\}$$

$$= \text{Tr} \left\{ \left(\sum_{k=1}^{M} I_{kx} \right) e^{-iH_0t} \rho(0) e^{iH_0t} \right\}. \qquad (2.4)$$

In the last line of Eq. (2.4) H_{hom} vanishes as a consequence of Eqs. (2.2) and (2.3), which means that $\rho(0)$ evolves only with H_0 and the homonuclear *J* coupling is not observable. While it can be readily shown that Eq. (2.2) is always valid, Eq. (2.3) is not fulfilled in general. Assuming the Hamilton operator of Eq. (2.1), a straightforward calculation leads to

$$[H_0, H_{\text{hom}}] = i2\pi \sum_{k=1, l=k+1}^{M} J_{Ik,Il}(\omega_{Ik} - \omega_{Il})(\vec{I}_k \times \vec{I}_l)_z. \quad (2.5)$$

Equation (2.5) implies that $[H_0, H_{\text{hom}}] = 0$ if $\omega_{Ik} = \omega_{Il}$ for all pairs of spins *k* and *l*. This is always the case in low field where the chemical shift differences are negligible small. Simulations of homonuclear coupled spins in low field show that the exact condition for which the homonuclear *J* coupling can be measured is given by

$$|\nu_{Ik} - \nu_{Il}| \geq |J_{Ik,Il}|, \qquad (2.6)$$

where the transition frequencies in Eq. (2.6) of spin *k* and *l* are defined as $\nu_{Ik} = \omega_{Ik}/(2\pi)$ and $\nu_{Il} = \omega_{Il}/(2\pi)$, respectively. In high magnetic fields (>1 T), Eq. (2.6) is always fulfilled since, for example, for protons the homonuclear *J*-coupling constants are ranging from $0.1-20$ Hz but the chemical shift differences of different chemical groups are a few ppm, typically more than 100 Hz. In contrast, in the Earth's magnetic field (5×10^{-5} T) the proton chemical shift differences are in the order of a few mHz, so $\nu_{Ik} \approx \nu_{Il} \approx \nu_I$. Therefore Eq. (2.6) is not fulfilled in the Earth's field and the homonuclear *J*-coupling is never expected to be measurable.

Consider a molecule of the form $X_N Y\text{-}AX_{M\text{-}N}$, which consists in *M* abundant spin 1/2 nuclei *X*, and one rare spin 1/2 nucleus *Y*. *X* is assumed to be the observed spin 1/2, *N* and *M-N* is the number of magnetically equivalent spins *X* of the chemical group $X_N Y$ and $AX_{M\text{-}N}$. The group *A* has no nuclear spin. It is possible to measure homonuclear *J* couplings if at least two additional heteronuclear *J*-couplings exist between the spins X_N and *Y* and between the spins $X_{M\text{-}N}$ and *Y*. We assume that the *M* spins *X* with angular momentum operator $\vec{I}_k$ $(k=1, \ldots, M)$ and the rare spin *Y* with angular momentum operator $\vec{S}$ interact with a low magnetic field. All spins *X* have the same Larmor frequency ω_I (no chemical shift differences) and the spin *Y* has the Larmor frequency ω_S. Defining $J_{Ik,S}$ as the heteronuclear *J*-coupling constants between spins $\vec{I}_k$ and $\vec{S}$ the Hamilton operator can be written as

$$H = \underbrace{\omega_I \sum_{k=1}^{M} I_{kz} + \omega_S S_z + 2\pi \sum_{k=1}^{M} J_{Ik,S} \vec{I}_k \cdot \vec{S}}_{H_{0,\text{het}}} + \underbrace{2\pi \sum_{k=1, l=k+1}^{M} J_{Ik,Il} \vec{I}_k \cdot I_l}_{H_{\text{hom}}},$$

(2.7)

where $H_{0,\text{het}}$ includes all heteronuclear *J*-coupling interactions. The homonuclear *J* coupling is not measurable if $[\Sigma_{k=1}^{M} I_{kx}, H_{\text{hom}}] = 0$ and if $[H_{0,\text{het}}, H_{\text{hom}}] = 0$. The second commutator is in general not equal to zero and can be expressed by

$$[H_{0,\text{het}}, H_{\text{hom}}] = i4\pi^2 \vec{S} \sum_{k=1, l=k+1}^{M} J_{Ik,Il}(J_{Il,S} - J_{Ik,S})(\vec{I}_k \times \vec{I}_l).$$

(2.8)

Equation (2.8) implies that if $J_{Il,S} \neq J_{Ik,S}$, then $[H_{0,\text{het}}, H_{\text{hom}}] \neq 0$, and the associated homonuclear *J*-coupling constant $J_{Ik,Il}$ is measurable. In analogy to Eq. (2.6), the exact condition for the measurement of the homonuclear *J*-coupling constant $J_{Ik,Il}$ is given by

$$|J_{Il,S} - J_{Ik,S}| \geq |J_{Ik,Il}|. \qquad (2.9)$$

The Eqs. (2.8) and (2.9) are the quantum mechanical equivalent formulation for the bead and spring model of homonuclear *J*-coupled spins [43]. Referring to the molecule $X_N Y - AX_{M\text{-}N}$, Eq. (2.9) means that the two different heteronuclear *J*-coupling constants $J_{Ik,S}$ $(k=1, \ldots, N)$ and $J_{Il,S}$ $(l = N+1, \ldots, M)$ break the magnetic equivalence between the spins $\vec{I}_k$ and $\vec{I}_l$, because the common transition frequency $\nu_I = \omega_I/(2\pi)$ of all *M* spins is changed by the two different heteronuclear *J*-couplings to $\nu_I \pm 0.5 J_{Ik,S}$ and to $\nu_I \pm 0.5 J_{Il,S}$.

B. The strongly coupled system YX_N

In this section it will be shown that in low field a chemical group YX_N (*Y*=rare spin 1/2, *X*=measured spin 1/2) with *N* magnetically equivalent spins *X* can be identified in the *X*-NMR spectrum even if the chemical shift and the homonuclear *J* coupling between the spins *X* cannot be measured. In low field the strong heteronuclear *J*-coupling regime, given by
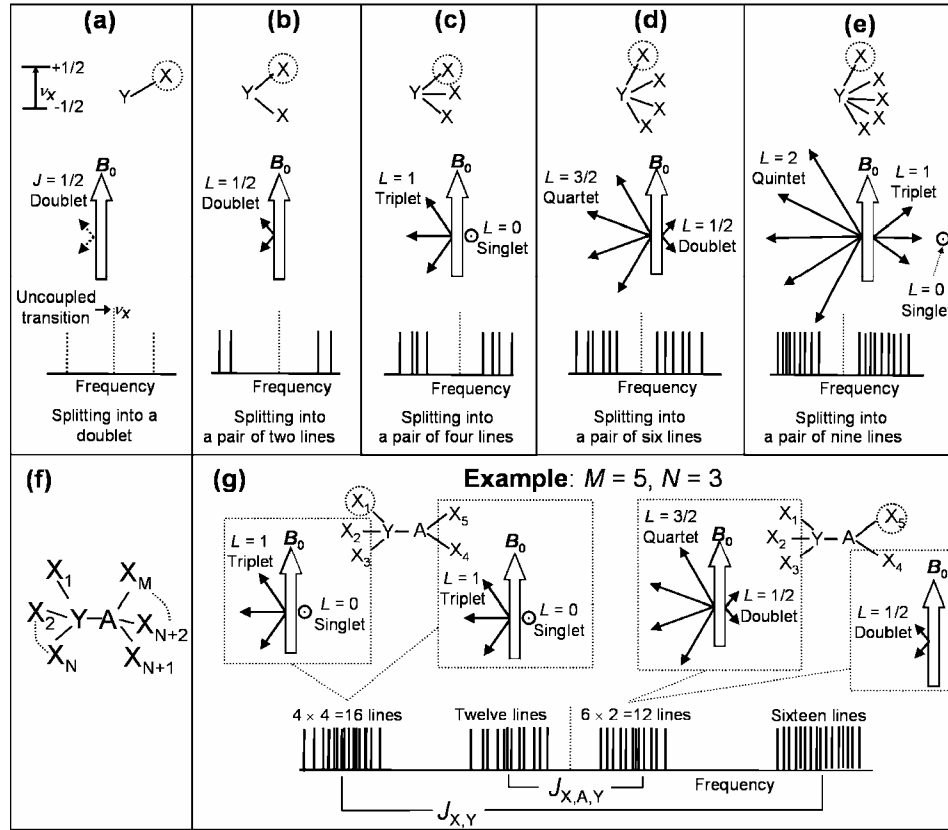
FIG. 1. Vector model of *J*-coupled *X* NMR in low field. (a)–(e) Schematic *X* spectrum of the strongly *J*-coupled YX_N group for $N=1$ to $N=5$. Dotted circle indicates the observed spin *X*. The splitting into multiplet lines is due to the transverse components of the total spin vector *L*. (f) Structure of the molecule $X_N Y$-$AX_{M\text{-}N}$. (g) Schematic homo- and heteronuclear *J*-coupled multiplet spectrum of the molecule $X_3 Y$-AX_2 and corresponding vector model.

$$1 \le |\nu_X - \nu_Y|/|J_{X,Y}| \le 100, \qquad (2.10)$$

is entered, where ν_X and ν_Y are the transition frequencies of the spins *X* and *Y* and $J_{X,Y}$ is the heteronuclear *J*-coupling constant. At high field the heteronuclear *J*-coupled *X* spectrum of the YX_N group is a pair of lines (a doublet) separated by $J_{X,Y}$. At low field the YX_N group can be distinguished by the splitting of each doublet line into *K* lines, where the natural number *K* is given by

$$K = \sum_{n=1, n \in U}^{N} 2(N-n)\frac{1}{2} + 1 = \sum_{n=1, n \in U}^{N} N-n+1. \quad (2.11)$$

U represents the set of odd numbers and *n* is a natural number. For example, a strongly coupled $^{13}CH_N$ group for $N=1$, 2, 3, 4 can be identified in the low field ^1H spectrum as a pair of one, two, four, and six *J*-coupled lines, respectively. Equation (2.11) can be explained by the vector model shown in Figs. 1(a)–1(e). If one specific spin *X* (dotted circle in Fig. 1) is picked out of the set of *N* identical spins *X*, then due to the strong heteronuclear *J* coupling the *X* spectrum splits first into an asymmetric pair of lines (a doublet) spaced by $J_{X,Y}$ [see Fig. 1(a)]. At low field the $N-1$ unobserved spins *X* couple into a combined total spin *L* which can have the values $L = (N-1)(1/2)$, $(N-3)(1/2)$, $(N-5)(1/2), \ldots , (N$

$-n)(1/2)$ for $n \in U$ until to $N-n=0$ for odd *N* or until to $N-n=1$ for even *N*. Each total spin *L* configuration has $2L+1$ possible spin orientations with respect to the magnetic field, as indicated for the YX_2, YX_3, YX_4, and YX_5 groups in Figs. 1(b)–1(e). The total number *K* of possible spin orientations is given by the sum over all $2L+1=2 \ (N-n)(1/2)+1$ spin orientations. Because the transverse components of all possible *L* cannot be neglected at low field each spin orientation of *L* leads to a different transition frequency and the resulting *X* spectrum is an asymmetric pair of *K* lines with different transition frequencies. Each transition frequency is related to the total spin state of the other $N-1$ spins *X*. At high field the transverse components of the $2L+1$ spin orientations can be neglected, all the *N* spins *X* are decoupled from each other, and all *K* lines collapse into a doublet line.

In order to investigate the predicted splitting in low field the *X*-NMR spectrum of the YX_N group for different values of *N* is simulated. Figure 2 shows the simulated *X* spectra of the YX_N group ($\nu_X=2000$ Hz, $J_{X,Y}=200$ Hz) for $N=1$, 2, 3, 4, and 5, respectively. The spectra show a single asymmetric doublet [Fig. 2(a)] and asymmetric pairs of two, four, six, and nine lines [Figs. 2(b)–2(e)], which is in full agreement with the prediction of Eq. (2.11).
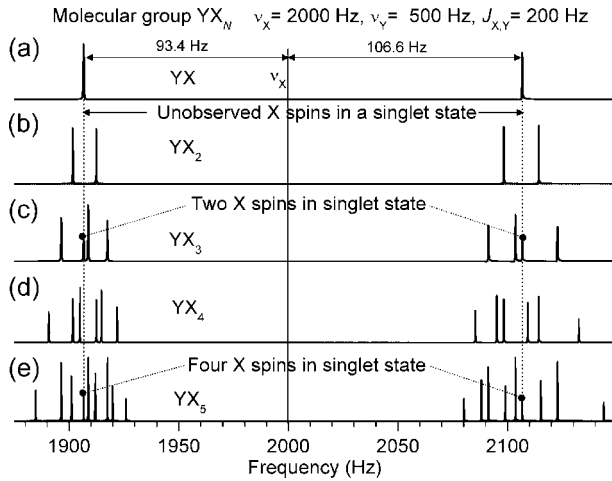
FIG. 2. Simulations of the Earth's field X-NMR spectrum of the strongly coupled YX_N group. The direct product approach was used to evaluate the $(2^{N+1} \times 2^{N+1})$-dimensional matrix representation in the Zeeman eigenbasis of the spin operators $\vec{I}_1, \vec{I}_2, \ldots, \vec{I}_N$ (the N spins X) and $\vec{S}$ (the Y spin). The initial density matrix at $t=0$ after a $90°$ y-pulse excitation is $\rho(0) = \Sigma_{k=1}^{N} I_{kx} + 0.25 S_x$. $\rho(t) = e^{-iHt} \rho(0) e^{iHt}$ with $H = \omega_I \Sigma_{k=1}^{N} I_{kz} + \omega_S S_z + 2\pi J_{I,S} \vec{S} \cdot \Sigma_{k=1}^{N} \vec{I}_k$ is calculated numerically. The free induction decay (FID) is obtained by the trace of the total transverse X spin multiplied with the density matrix. After Fourier transformation of the FID the spectrum is phase corrected. A global transverse relaxation time (linewidth of 0.1 Hz) is introduced such that the essential spectral features are well resolved.

C. Spin singlets and reduced spin relaxation rate

The two dotted lines in Fig. 2 indicate the position of the two transitions of the YX_N group where for $N=3$, the $N-1=2$ spins X are coupled into a singlet and for $N=5$, the $N-1=4$ spins X are coupled into a pair of singlets. For $N=3$ the two initial wave functions $\Psi_{S,3}^{\text{up}}$ and $\Psi_{S,3}^{\text{down}}$ can be expressed in the basis of the up and down eigenstates $|\uparrow\rangle$ and $|\downarrow\rangle$ of the I_{kz} ($k=1,2,3$) operator as

$$\Psi_{S,3}^{\text{up}} = 1/\sqrt{2}[|(\uparrow\downarrow)_{1,2}\uparrow\rangle - |(\downarrow\uparrow)_{1,2}\uparrow\rangle],$$

$$\Psi_{S,3}^{\text{down}} = 1/\sqrt{2}[|(\uparrow\downarrow)_{1,2}\downarrow\rangle - |(\downarrow\uparrow)_{1,2}\downarrow\rangle]. \quad (2.12)$$

The third spin outside the round brackets indicates the state of the observed nucleus X. The common term $1/\sqrt{2}[|(\uparrow\downarrow)_{1,2}\rangle - |(\downarrow\uparrow)_{1,2}\rangle]$ in Eq. (2.12) represents a spin-singlet state of the spins at position 1 and 2. $\Psi_{S,3}^{\text{up}}$ and $\Psi_{S,3}^{\text{down}}$ are antisymmetric with respect to the exchange between the two spins at the positions 1 and 2. Two other wave functions analogous to Eq. (2.12) can be constructed where spin 1 and 3 or spin 2 and 3 are coupled into a singlet and the remaining spin is observed. The expectation value of the total magnetic moment associated with the coupled singlet is zero. This singlet state has no dipole-dipole interaction or J coupling with the observed spin X and narrow linewidths are expected.

It can be shown that for $N=5$ the $N-1=4$ spins cannot be described by an antisymmetric four spin singlet wave function. If the position of each of the four spins X is numerated

by 1, 2, 3, 4, and spin 1 and 2 as well as spin 3 and 4 each couple into a spin singlet, the initial five spin wave function for the case where the measured spin X is in the up state is given by

$$\Psi_{S,5}^{\text{up}} = \frac{1}{2}[|(\uparrow\downarrow)_{1,2}(\uparrow\downarrow)_{3,4}\uparrow\rangle - |(\uparrow\downarrow)_{1,2}(\downarrow\uparrow)_{3,4}\uparrow\rangle$$
$$- |(\downarrow\uparrow)_{1,2}(\uparrow\downarrow)_{3,4}\uparrow\rangle + |(\downarrow\uparrow)_{1,2}(\downarrow\uparrow)_{3,4}\uparrow\rangle]. \quad (2.13)$$

An analogous wave function $\Psi_{S,5}^{\text{down}}$ can be defined if the measured spin X is in the down state. The two other possible pairs of wave functions can be constructed for $(i,j,k,l) = (1,3,2,4)$ or $(1,4,2,3)$. $\Psi_{S,5}^{\text{up}}$ is antisymmetric with respect to the exchange of $(i,j)=(1,2)$ or $(k,l)=(3,4)$. Because the expectation value of the total magnetic moment of the two singlet pairs in Eq. (2.13) is zero, the dipolar field of the four coupled spins at the position of the observed spin X is reduced or even zero, depending on the relative position of the measured spin X. Therefore, for the pair of singlets in the YX_5 molecule both the longitudinal and transverse relaxation times of the measured spin X are expected to be significantly longer than those of the other spin states.

D. *J*-coupled nuclear magnetic resonance spectrum of the molecule $X_N Y\text{-}AX_{M\text{-}N}$

What is the structure of the J-coupled X-NMR spectrum in low field for the general case of a molecule $X_N Y\text{-}AX_{M\text{-}N}$ [see Fig. 1(f)]? Figure 1(g) shows, for example, the spectrum of the molecule $X_3 Y\text{-}AX_2$, which is characterized by two heteronuclear J-coupling constants, $J_{X,Y}$ and $J_{X,A,Y}$, and by the homonuclear coupling constant $J_{X,X}$ between the $X_3 Y$ and the AX_2 group. According to Eq. (2.8) the homonuclear coupling constant between the X spins within the $X_3 Y$ and the AX_2 group is not measurable, but the homonuclear constant $J_{X,X}$ is observable if Eq. (2.9) is valid. Assuming $|J_{X,Y}| > |J_{X,A,Y}| > |J_{X,X}|$ and that the two strong coupling conditions $1 \leq |\nu_X - \nu_Y|/|J_{X,Y}| \leq 100$ and $1 \leq |J_{X,Y} - J_{X,A,Y}|/|J_{X,X}| \leq 100$ are valid, the X-NMR spectrum of the YX_3 group is a pair of sixteen lines while the X spectrum of the AX_2 group is a pair of twelve lines, as indicated in Fig. 1(g). According to the vector model the X-NMR spectrum of the $X_3 Y$ group alone is a pair of four lines. Each of these four lines splits into four lines, due to the strong homonuclear J coupling between the $X_3 Y$ and the AX_2 group. Therefore a pair of multiplets with sixteen lines each spaced by $J_{X,Y}$, is expected. On the other side the X-NMR spectrum of the strongly homonuclear coupled AX_2 system in the molecule is a pair of two lines [see Fig. 1(b)]. Each of these lines splits into six lines, due to the strong homonuclear coupling $J_{X,X}$ between the AX_2 and the $X_3 Y$ group [Fig. 1(g)]. Thus the total X-NMR spectrum of the AX_2 group is a pair of twelve multiplet lines spaced by $J_{X,A,Y}$.

Table I shows for the $X_N Y\text{-}AX_{M\text{-}N}$ molecule how to calculate the number of lines of each multiplet for four different cases of weak and strong J couplings. We assume two heteronuclear J-coupling conditions [(1) coupling conditions in Table I], which depend on the magnetic field and one field independent homonuclear J-coupling condition [(2) coupling condition]. If all three coupling conditions are weak (case 1)

TABLE I. Number of lines for the pair of multiplets for the molecule $X_N Y$-AX_{M-N}.

Case	(1) coupling condition	(2) coupling condition	Number of lines for the N spins X	Number of lines for the M-N spins X
1	$\begin{array}{l} \lvert \nu_X - \nu_Y \rvert / \lvert J_{X,Y} \rvert > 100 \\ \lvert \nu_X - \nu_Y \rvert / \lvert J_{X,A,Y} \rvert > 100 \\ \text{both weak} \end{array}$	$\begin{array}{l} \lvert J_{X,Y} - J_{X,A,Y} \rvert / \lvert J_{X,X} \rvert > 100 \\ \text{weak} \end{array}$	$2(M-N+1)$	$2(N+1)$
2	$\begin{array}{l} 1 \le \lvert \nu_X - \nu_Y \rvert / \lvert J_{X,Y} \rvert \le 100 \\ \lvert \nu_X - \nu_Y \rvert / \lvert J_{X,A,Y} \rvert > 100 \\ \text{strong, weak} \end{array}$	$\begin{array}{l} \lvert J_{X,Y} - J_{X,A,Y} \rvert / \lvert J_{X,X} \rvert > 100 \\ \text{weak} \end{array}$	$2(M-N+1) \times \displaystyle\sum_{n=1,\,n\in U}^{N}(N-n+1)$	$2(N+1)$
3	$\begin{array}{l} 1 \le \lvert \nu_X - \nu_Y \rvert / \lvert J_{X,Y} \rvert \le 100 \\ 1 \le \lvert \nu_X - \nu_Y \rvert / \lvert J_{X,A,Y} \rvert \le 100 \\ \text{both strong} \end{array}$	$\begin{array}{l} \lvert J_{X,Y} - J_{X,A,Y} \rvert / \lvert J_{X,X} \rvert > 100 \\ \text{weak} \end{array}$	$2 \displaystyle\sum_{n=1,\,n\in U}^{N}(N-n+1) \times \displaystyle\sum_{m=0,\,m\in G}^{M-N}(M-N-m+1)$	$2 \displaystyle\sum_{n=1,\,n\in U}^{M-N}(M-N-n+1) \times \displaystyle\sum_{m=0,\,m\in G}^{N}(N-m+1)$
4	$\begin{array}{l} 1 \le \lvert \nu_X - \nu_Y \rvert / \lvert J_{X,Y} \rvert \le 100 \\ 1 \le \lvert \nu_X - \nu_Y \rvert / \lvert J_{X,A,Y} \rvert \le 100 \\ \text{both strong} \end{array}$	$\begin{array}{l} 1 \le \lvert J_{X,Y} - J_{X,A,Y} \rvert / \lvert J_{XX} \rvert \le 100 \\ \text{strong} \end{array}$	$2 \displaystyle\sum_{n=1,\,n\in U}^{N}(N-n+1) \times \displaystyle\sum_{m=0,\,m\in G}^{M-N}(M-N-m+1)$	$2 \displaystyle\sum_{n=1,\,n\in U}^{M-N}(M-N-n+1) \times \displaystyle\sum_{m=0,\,m\in G}^{N}(N-m+1)$

a symmetric pair of $(M-N+1)$ lines is observed in the X spectrum for the $X_N Y$ group and a symmetric pair of $(N+1)$ lines for the AX_{M-N} group. In case 2, where the $X_N Y$ group is strongly coupled and the other two coupling conditions are weak, the spectrum for the AX_{M-N} group remains as a pair of $(N+1)$ lines while the spectrum of the $X_N Y$ group splits into a pair of $(M-N+1)\sum_{n=1,n\in U}^{N}(N-n+1)$ lines. If both groups $X_N Y$ and AX_{M-N} are strongly heteronuclear coupled (case 3) or the strong homonuclear coupling condition is valid (case 4) the number of lines is given by the product of two factors as shown in Table I.

E. Line intensities of *J*-coupled multiplet lines

The expected intensities of the homo- and heteronuclear *J*-coupled multiplet lines of the molecule $X_N Y$-AX_{M-N} can be estimated for case 1 in Table I. The intensity A_{N+1} of the smallest line of the $N+1$ multiplet is given by

$$A_{N+1} = A_0 f \frac{1}{2} \frac{M-N}{M} \frac{1}{2^N}, \qquad (2.14)$$

and the intensity A_{M-N+1} of the smallest line from the $M-N+1$ multiplet is

$$A_{M-N+1} = A_0 f \frac{1}{2} \frac{N}{M} \frac{1}{2^{M-N}}. \qquad (2.15)$$

A_0 is defined as the intensity of the observed uncoupled X line, and f is the abundance of the rare spin Y. For example, if Y corresponds to ^{13}C in natural abundance ($f=0.01$) the intensity of the smallest multiplet line is more than 1000 times smaller than A_0. The detection of a multiplet spectrum with ^{13}C in natural abundance requires a very sensitive spectrometer and narrow linewidths.

III. EXPERIMENTAL SETUP

The ^{1}H-NMR spectra of the following molecules were measured with coil based low field and Earth's field NMR: hypophosphinic acid (50% H_3PO_2 + 50% H_2O) as an example for a strongly coupled YX_2 group ($Y = ^{31}$P, $X = ^1$H), 99% ^{13}C-enriched methanol as an example for the molecule YX_3 group ($Y = ^{13}$C, $X = ^1$H), and 99% ^{13}C-enriched ethanol. For ethanol in one case the methyl group (ethanol II: $X_3 Y$-AX_2-BX with $A = ^{12}$C, $B = ^{16}$O, $Y = ^{13}$C, $X = ^1$H) and in the other case the methylene group (ethanol I: $X_3 A$-YX_2-BX) was selectively enriched. Advantages of coil based detection of NMR signals in low fields are the simplicity and that the NMR lines are practically not broadened in the Earth's magnetic field. The linewidth is expected to be very narrow because it is dominated by the natural transverse relaxation time T_2 of the observed nuclear spins. Figure 3 shows the experimental setup for the measurements at low field (left) and in the Earth's magnetic field (right).

A. Low field NMR

The magnetic field (2×10^{-4}–2×10^{-2} T) is produced by a cylindrical solenoid, using a homemade current supply
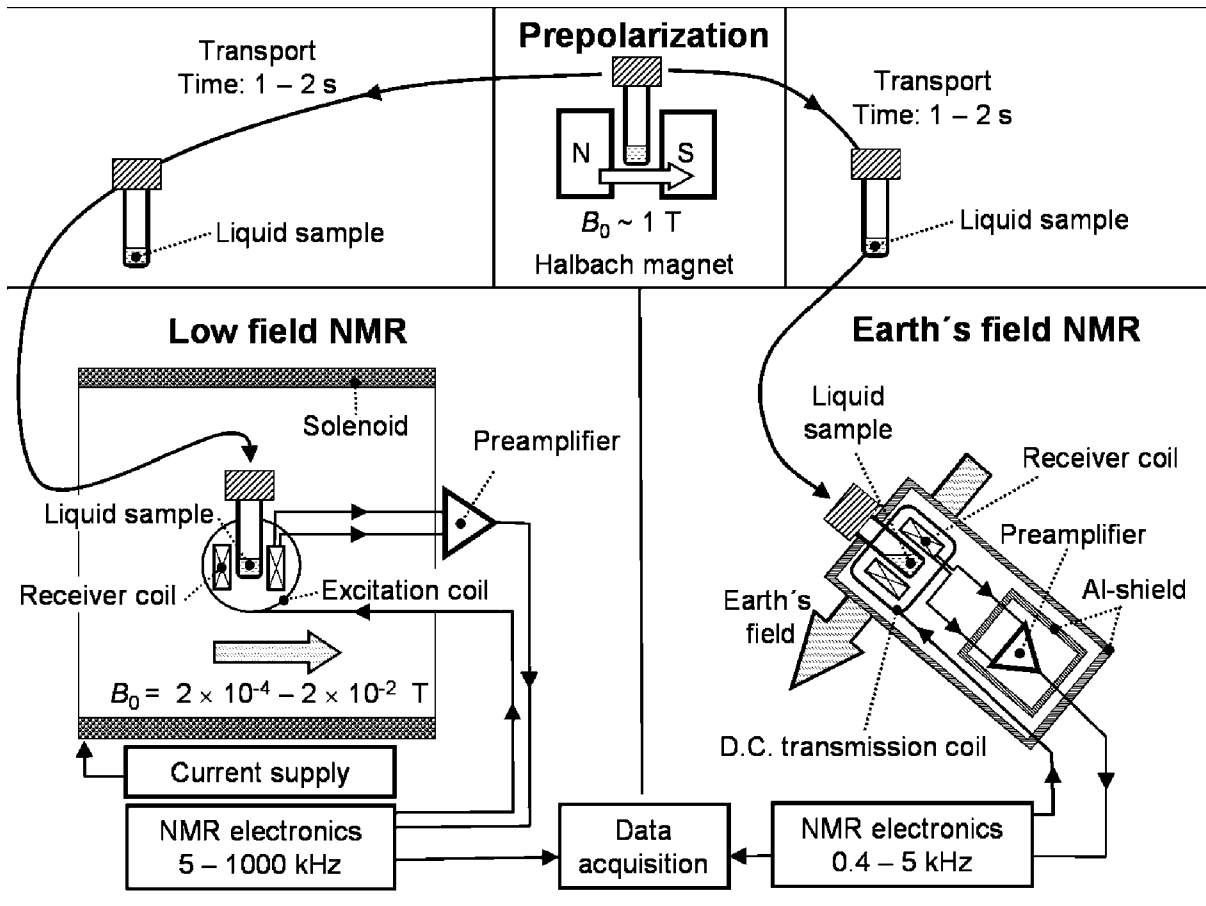
FIG. 3. Setup for NMR measurements at low field (left) and in the Earth's field (right). Top: prepolarization of the sample in a 1 T Halbach magnet for both experiments.

(stability ~ 1 ppm h^{-1}). After premagnetization, the sample (~ 0.25 cm^3) is transferred into a receiver coil (solenoid) with an inner diameter of 10.5 mm. For excitation of the spins a separate saddle coil is used. The receiver coil can be tuned to any resonance frequency between 5–1000 kHz, depending on the adjusted B_0-field value. The resulting NMR signal is amplified by the preamplifier, processed by the NMR electronics, and evaluated. The field homogeneity of the B_0 field is about 10^{-4} cm^{-1}.

B. Earth's field nuclear magnetic resonance

The Earth's field spectrometer is shielded by a 20 mm aluminum cylinder against ambient electromagnetic noise. The transverse magnetization is generated by a 90° dc magnetic field pulse with the saddle coil, the subsequent free induction decay (FID) is measured by a NMR receiver coil which is tuned to the resonance frequency of the protons in the Earth's field (~ 2 kHz). The NMR spectrometer is operating close to the Johnson noise limit. For sample preparation 2 cm^3 of the liquid sample is filled in a NMR glass tube with a valve. All samples are deoxygenated by several freezing and thawing cycles under high vacuum conditions. Finally, the samples are flushed with ^{4}He gas at a few bars pressure, and the valve is closed. Typical measured ^{1}H line-

widths in the Earth's field are between 0.03–0.3 Hz. More detailed information of the Earth's field NMR spectrometer can be found in [42,43].

C. Measurement procedure

For both experimental setups the premagnetization of the sample is carried out by a 1 T Halbach permanent magnet [42] (Fig. 3, top) composed of eight magnetized FeNd segments. The weak stray field outside the magnet typically broadens a proton NMR line at 1 m distance to about 0.1 Hz. This broadening is avoided by increasing the distance between the Halbach magnet and the NMR probe to several meters. After the premagnetization the sample is carried within 1–2 s into the low field probe or into the Earth's field NMR probe.

IV. EXPERIMENTAL RESULTS

A. Strongly *J*-coupled low-field nuclear magnetic resonance of the groups YX_2 and YX_3

1. $^{31}PH_2$ group

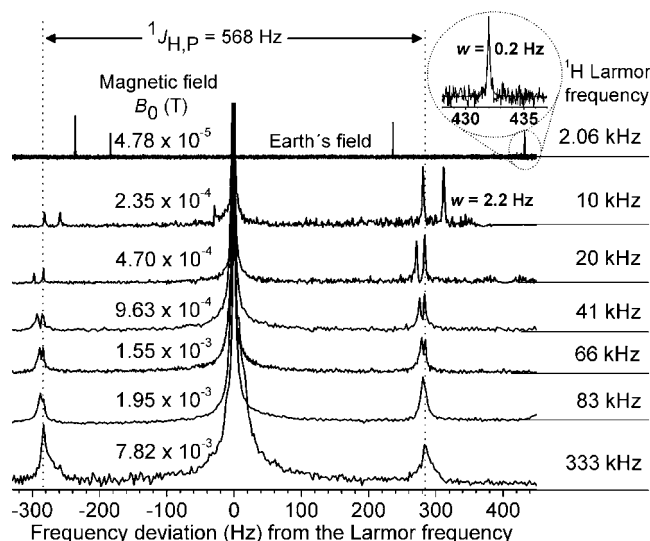One example for a strongly *J*-coupled YX_N group with $N=2$ is the $^{31}PH_2$ group. The ^{1}H-NMR spectrum of the

FIG. 4. Low and Earth's field ^{1}H spectra of the ^{31}PH$_2$ group. The Larmor frequency (magnetic field) is the parameter of the spectra. A splitting into a pair of two lines starts to be visible below 83 kHz. Insert in the top: Enhanced view of one line of the Earth's field spectrum. The linewidths of the low field NMR spectra are determined by the B_0 field inhomogeneity while the width of the Earth's field spectrum is given by the T_2 relaxation time of the sample.

^{31}PH$_2$ group can be observed in a solution of H$_3$PO$_2$ in water. The PH$_2$ group is stable whereas the OH proton of H$_3$PO$_2$ rapidly exchanges with the water molecule. Therefore the *J* coupling of all mobile protons (the protons of H$_2$O and the OH proton of H$_3$PO$_2$) is averaged out and appears in the NMR spectrum as an uncoupled ^{1}H line. The *J*-coupling constant between ^{31}P (γ_P=17.236 MHz T^{-1}) and ^{1}H (γ_H =42.576 MHz T^{-1}) is $^1J_{H,P}$=568 Hz. With these values the condition for strong *J* coupling is fulfilled if the B_0 field is smaller than about 2×10^{-3} T ($\nu_H\sim$ 85 kHz). First measurements and theoretical calculations of the ^{31}PH$_2$-NMR spectrum in the range of the Earth's field were reported by Benoit *et al.* [6]. In Fig. 4 we show the ^{1}H spectra for the ^{31}PH$_2$ group in the field regime from 7.8×10^{-3} T (333 kHz) down to the Earth's field (4.78×10^{-4} T). From the theory we expect for the *J*-coupled YX_2 system in high field a *J*-coupled doublet and in low field a pair of two lines. In Fig. 4 below 83 kHz the strong coupling limit $1\leq|\nu_H-\nu_P|/|^1J_{H,P}|\approx89$ <100 is entered and the experimental line profile shows a first indication of a splitting into a pair of two lines. The splitting and the asymmetry (relative to the Larmor frequency) of the lines increase with the decreasing magnetic field and are in excellent agreement with the theory. The uncoupled ^{1}H line in Fig. 4 is set as reference and as the zero deviation from the Larmor frequency at the corresponding field. The linewidths of the *J*-coupled lines decreases from about 10 Hz at 333 kHz to the natural linewidth at the Earth's field (2.06 kHz), which is 0.2 Hz. In most Earth's field NMR experiments the contribution of line broadening due to the inhomogeneity of the Earth's field is negligible small compared to the natural linewidth.
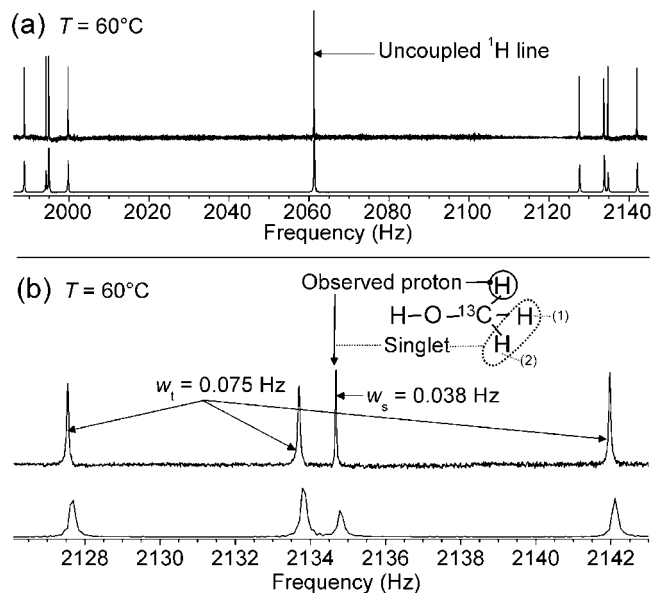

FIG. 5. Experimental and simulated *J*-coupled Earth's field ^{1}H spectra of 99% ^{13}C enriched methanol. The dotted line in the methanol molecule indicates the two protons which can be either in a singlet or a triplet state. For the experimental spectrum [Fig. 5(a), top] nine scans are averaged. The ^{1}H spectrum measured at T =60 °C shows a pair of four unevenly spaced lines. The simulation of the spectrum with a linewidth of 0.16 Hz is shown in the bottom. (b) Enhanced view of the right multiplet of the spectrum. The experimental spectrum [Fig. 5(b), top] consists in one narrow line (w_s=0.038 Hz) and three broad lines (w_t=0.075 Hz). Bottom: The simulation is in good agreement with the experimental spectrum except for the linewidth (0.16 Hz).

2. ^{13}CH$_3$ group

The strongly *J*-coupled ^{1}H-NMR spectrum of a ^{13}CH$_3$ group is investigated with 99% ^{13}C- enriched methanol (^{13}CH$_3$OH) at a temperature of T=60 °C. Under these conditions the protons of the OH group of methanol exchange so rapidly between different molecules that they do not experience any homo- or heteronuclear *J* couplings. Therefore the *J*-coupled ^{1}H-Earth's field spectrum of enriched methanol is an example of a strongly coupled four-spin system YX_3 with one ^{13}C and three protons. In the top of Fig. 5(a) is shown the pair of four lines with an asymmetric pattern and varying line spacing. The measured spectrum is in full agreement with the simulation of the strongly coupled ^{13}CH$_3$ group [Fig. 5(a), bottom] assuming $^1J_{H,C}$=140.6 Hz [43,44]. The uncoupled protons are visible in the ^{1}H spectrum by the central line at 2061.29 Hz. We conclude from the low field ^{1}H spectra of the ^{31}PH$_2$ and ^{13}CH$_3$ group that the specific chemical group can be unambiguously identified from the number of lines without the need of any chemical shift information.

Let us analyze the linewidths of one multiplet. Figure 5(b) shows an enhanced view of the right multiplet of Fig. 5(a). For the experimental spectrum [Fig. 5(b), top] the width w_s =0.038 Hz of the line at 2134.65 Hz is about a factor 2 smaller compared to the width w_t=0.075 Hz of the other three lines. The narrow line is associated to a singlet state of
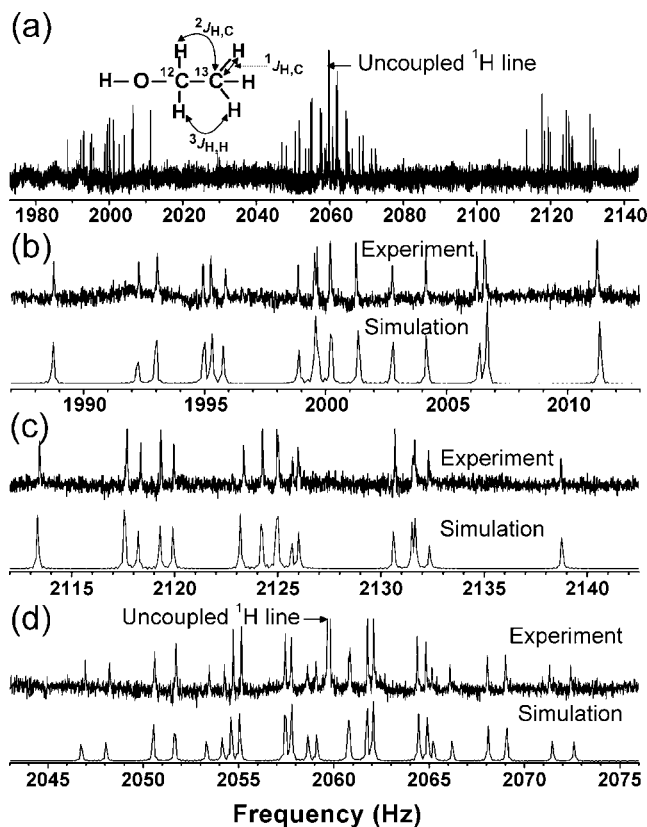
FIG. 6. *J*-coupled Earth's field ^{1}H spectra of ethanol II (99% ^{13}C enriched at the CH$_3$ group) at $T=60$ °C. (a) Complete experimental spectrum measured at $B_0=4.8378\times10^{-5}$ T (2059.76 Hz) with a single scan. The linewidth of all the *J*-coupled lines is ~0.05 Hz. (b) and (c), top: Enhanced view of the experimental spectra of the strongly coupled outer pair consisting of sixteen unevenly spaced lines each. Bottom: Simulated spectra of the outer pair of multiplets. (d), top: Enhanced view of the experimental spectrum of the weakly coupled inner pair consisting of twelve unevenly spaced lines each. Bottom: Simulated spectrum of the inner pair of multiplets. The simulated linewidths are all 0.08 Hz. Not all of the *J*-coupled lines in Figs. 6(b)–6(d) are resolved in the presented spectra.

two protons in the ^{13}CH$_3$ group with an associated three spin wave function expressed by Eq. (2.12). The other three lines correspond to the triplet state of two protons in the ^{13}CH$_3$ group. The singlet line is narrow because the proton spin singlet has no magnetic moment and thus has a reduced or zero intramolecular dipole-dipole interaction with the observed proton. A similar phenomenon is reported by Carravetta *et al.* [45,46], who measured with the field-cycling method in low field a prolonged longitudinal spin relaxation time T_1 of a singlet-spin state. In contrast to Carravetta, we observe here directly in the Earth's field a prolonged transverse relaxation time.

B. Observation of homo- and heteronuclear *J* couplings in low field

1. Ethanol II: HO-^{12}CH$_2$-^{13}CH$_3$

In the following the *J*-coupled ^{1}H-Earth's field spectrum of two molecular groups bound together is discussed. As an
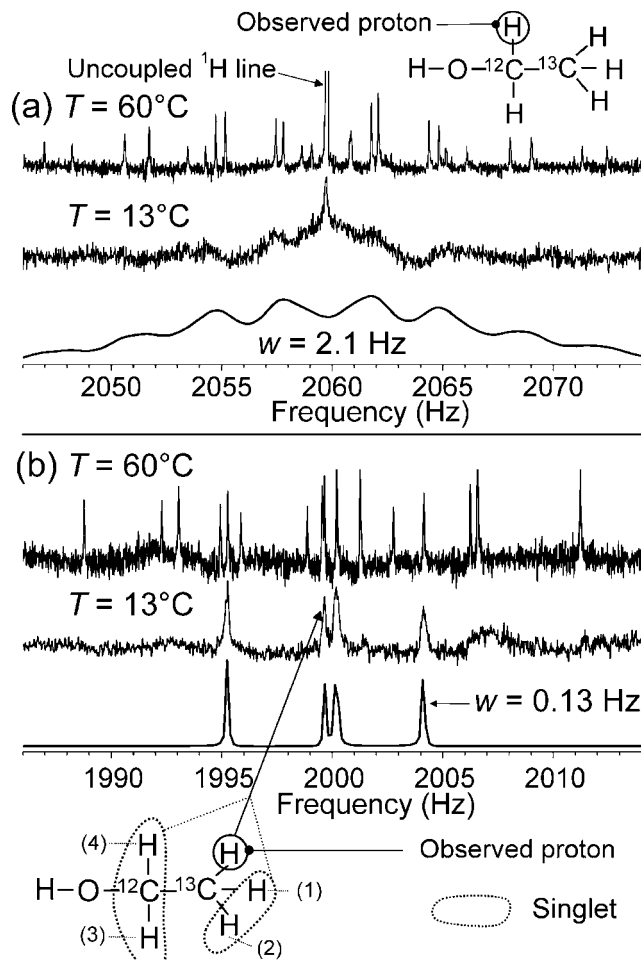

FIG. 7. Comparison of *J*-coupled Earth's field ^{1}H spectra of ethanol II at $T=60°$ and 13 °C. Nine scans have been averaged. (a) NMR spectrum of the weakly coupled inner pair of multiplets at $T=60$ °C (top) and $T=13$ °C (middle). Bottom: Simulated spectrum for 13 °C assuming a linewidth of $w=2.1$ Hz. (b) NMR spectra of the strongly coupled left outer multiplet, consisting of sixteen lines at $T=60$ °C (top) and of four lines at $T=13$ °C (middle). From the sixteen lines only four lines (three triplet lines and one singlet line) remain. Bottom: Simulation of the ^{1}H spectrum of the strongly heteronuclear coupled ^{13}CH$_3$ group with $^1J_{H,C}=125.2$ Hz.

example ^{13}C-enriched ($f=0.99$) ethanol II (HO-^{12}CH$_2$-^{13}CH$_3$) is investigated, where II means the position of the ^{13}C spin at the CH$_3$ group. The intermolecular proton exchange of the ethanol molecules gives rise to an uncoupled ^{1}H line of the OH group, which does not participate in the *J*-coupled network. Therefore, for ethanol six *J*-coupled spins need to be considered with the molecular structure X_NY-$AX_{M\text{-}N}$ with $X=^1$H, $Y=^{13}$C, $A=^{12}$C, $M=5$, and $N=3$. From the high-field NMR spectrum of ethanol it is known that $^1J_{H,C}=124.9$ Hz, $^2J_{H,C}=-2.5$ Hz, and $^3J_{H,H}=6.9$ Hz [44,47]. In the Earth's field the weak coupling condition $|\nu_H-\nu_C|/|^2J_{H,C}|\approx700>100$ and the two strong coupling conditions $1\leq|\nu_H-\nu_C|/|^1J_{H,C}|\approx13\leq100$ and $1\leq|^1J_{H,C}-^2J_{H,C}|/|^3J_{H,H}|\approx17\leq100$ are valid, so we have case 4 of Table I. Figure 6(a) shows the total Earth's field ^{1}H spectrum of HO-^{12}CH$_2$-^{13}CH$_3$ consisting of an inner and an

outer multiplet pair. An enhanced view of the outer multiplet pair centered at ± 0.5 $^{1}J_{H,C}$ is shown in Figs. 6(b) and 6(c). Sixteen unevenly spaced lines for each multiplet are identified as predicted by the theory in Table I, case 4. The inner multiplet pair centered at ± 0.5 $^{2}J_{H,C}$ around the uncoupled ^{1}H line is shown in Fig. 6(d). Twelve lines for each inner multiplet are visible. The simulations in the bottom of Figs. 6(b)–6(d) of the six-spin system fit perfectly with all experimentally observed lines if we set 2059.76 Hz for the frequency of the uncoupled protons and $^{1}J_{H,C}=125.2$ Hz, $^{2}J_{H,C}=-2.4$ Hz, and $^{3}J_{H,H}=7.1$ Hz. These values for $^{1}J_{H,C}$, $^{2}J_{H,C}$, and $^{3}J_{H,H}$ are in full agreement with the literature values [44,47].

How does the linewidth of the ^{1}H-NMR spectrum of ethanol II depend on the temperature and on the spin state of the molecule? The main transverse relaxation is caused by the modulation of the intra- and intermolecular dipole-dipole interaction due to the intramolecular rotation and due to intermolecular collisions. In Fig. 7 the *J*-coupled ^{1}H-NMR spectra of ethanol II are shown at two different temperatures, $T=60$ °C and 13 °C. In the top of Fig. 7(a) the spectrum at 60 °C shows the inner pair of multiplets, with twelve narrow lines for each multiplet. The lines are narrow because at 60 °C the correlation times of the dipole-dipole interactions are short. At $T=13$ °C [Fig. 7(a), middle] the viscosity is higher and the correlation times are longer, so intra- and intermolecular dipole-dipole interactions cause a significant line broadening ($w \sim 2$ Hz). Only the relative narrow uncoupled ^{1}H line ($w \sim 0.2$ Hz) at 2059.76 Hz can be identified. If one $^{12}CH_2$ proton is observed then according to the vector model (Fig. 1) no singlet state exists in the $^{12}CH_2$ and in the $^{13}CH_3$ group. Therefore narrow lines are not expected to be observed at 13 °C. The simulation in the bottom of Fig. 7(a) shows the essential features of the experimental spectrum at 13 °C if a linewidth of 2.1 Hz is assumed.

The situation is completely different if the observed proton is located at the $^{13}CH_3$ group, as shown in Fig. 7(b). At $T=60$ °C (top) sixteen narrow lines ($w \sim 0.05$ Hz) are observed, as already discussed in Fig. 6(b). At 13 °C (middle) only four of the sixteen lines survive, and these four lines are exactly at the same frequency positions as the lines expected from the strongly coupled $^{13}CH_3$ group of ethanol II with no homonuclear *J* coupling to the $^{12}CH_2$ group. This is proved by the simulation of the four-spin system $^{13}CH_3$ at the bottom of Fig. 7(b), assuming $^{1}J_{H,C}=125.2$ Hz. The experimental spectrum (middle) consists of three broader triplet lines ($w_t \sim 0.23$ Hz) and one narrower singlet line ($w_s \sim 0.16$ Hz) similar to the methanol spectrum in Fig. 5. The survival of the four lines can be explained by the existence of a singlet state of the two protons of the $^{12}CH_2$ group. The other twelve lines in the spectrum are not visible because of strong dephasing for those ethanol molecules, for which the $^{12}CH_2$ group is in the triplet state. The $^{12}CH_2$ singlet state has two effects: (1) The homonuclear *J* coupling between the $^{13}CH_3$ and the $^{12}CH_2$ groups is zero. (2) The $^{12}CH_2$ group has no magnetic moment so the intramolecular dipole-dipole relaxation rate between the rotating $^{12}CH_2$ and $^{13}CH_3$ groups is reduced significantly. For the singlet line [indicated by an arrow in Fig. 7(b)], the two protons in the $^{13}CH_3$ group are
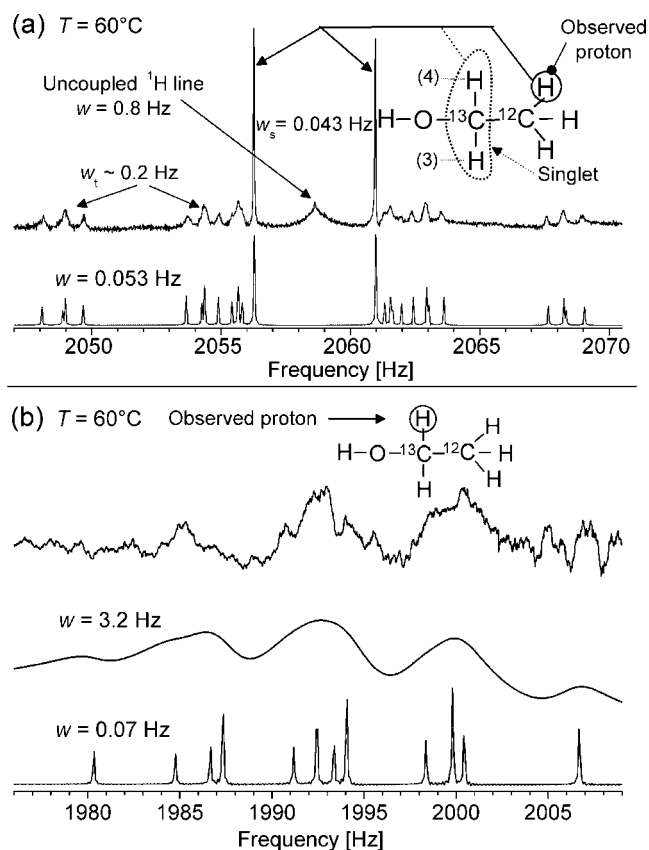

(a) $T = 60$°C

Uncoupled ^{1}H line
$w = 0.8$ Hz
$w_s = 0.043$ Hz
$w_t \sim 0.2$ Hz
Observed proton
Singlet
$w = 0.053$ Hz
2050   2055   2060   2065   2070
Frequency [Hz]

(b) $T = 60$°C   Observed proton
$w = 3.2$ Hz
$w = 0.07$ Hz
1980   1985   1990   1995   2000   2005
Frequency [Hz]

FIG. 8. *J*-coupled ^{1}H-Earth's field spectra of ethanol I at $T=60$ °C. Each spectrum is an average over nine scans. (a) Top: Enhanced view of the experimental spectrum of the inner pair of multiplets consisting of thirteen resolved unevenly spaced lines each. Bottom: Simulated spectrum of the inner pair of multiplets assuming a linewidth of 0.053 Hz. See text for the simulation parameters. (b) Top: Experimental spectrum of the outer multiplet at 1976–2009 Hz. The outer multiplet consists of very broad unstructured lines with a width of about 3 Hz. Middle: Simulated spectrum of the outer left multiplet ($w \sim 3.2$ Hz). Bottom: The simulated, highly resolved spectrum assuming a line width of 0.07 Hz.

also in the singlet state. Therefore also the dipole-dipole interaction within the $^{13}CH_3$ group is reduced, and the linewidth is narrower than that of the triplet lines. This is a demonstration of a two-pair singlet state, where the dipole interaction of four protons with the observed proton is significantly suppressed.

2. Ethanol I: HO-$^{13}CH_2$-$^{12}CH_3$

Figure 8 shows the *J*-coupled Earth's field NMR spectrum of the six-spin system ethanol I (HO-$^{13}CH_2$-$^{12}CH_3$), where the methylene group is 99% enriched with ^{13}C. The formal molecular structure is $X_N Y$-AX_{M-N} with $X=^{1}$H, $Y=^{13}$C, $A=^{12}$C, $M=5$, $N=2$. In contrast to the case of ethanol II the protons of the $^{12}CH_3$ group are weakly and the protons of the $^{13}CH_2$ group are strongly heteronuclear *J* coupled to ^{13}C and the strong coupling condition $1 \leq |^{1}J_{H,C}-^{2}J_{H,C}|/|^{3}J_{H,H}| \leq 100$ still holds. This corresponds to case 4 of Table I, therefore the ^{1}H-NMR spectrum of the $^{12}CH_3$ group is ex-

pected to be of a pair of multiplets with sixteen lines each. The corresponding spectrum for the inner pair of multiplets is shown in Fig. 8(a). The broad multiplet lines (width w_t ~ 0.2 Hz) and the two narrow and intense lines (w_s $=0.043$ Hz) are grouped around the broad uncoupled ^{1}H line ($w \sim 0.8$ Hz). The simulated spectrum (parameters: $^1J_{H,C}$ $=140.4$ Hz, $^2J_{H,C}=-4.6$ Hz, $^3J_{H,H}=7.1$ Hz [47]) at the bottom of Fig. 8(a) shows a pair of sixteen lines where, for example, on the right side of the spectrum thirteen lines are resolved and the intense line is a superposition of four lines. Because the weak coupling condition $|\nu_H-\nu_C|/|^2J_{H,C}|$ >100 holds, the signal does not split into four lines [such as in Fig. 7(b)], but the lines superpose to form one intense line.

In Fig. 8(b), the left of the two outer multiplets shows very broad structures ($w \sim 3$ Hz). The measured spectrum is approximated by the simulation shown in the middle trace assuming that each line of the well resolved simulated multiplet structure [see Fig. 8(b), bottom] is strongly broadened ($w=3.2$ Hz). Why are the lines at $T=60$ °C of the ^{13}CH$_2$ group so extremely broad compared to the narrow lines of the ^{12}CH$_2$ group in Fig. 7(a)? Besides the dipole-dipole interaction another relaxation mechanism is the transverse ^{1}H relaxation of the ^{13}CH$_2$ protons due to slow proton exchange ($\tau_r \sim 10-100$ ms) of the OH group. This proton exchange strongly dephases the coherence of the ^{13}CH$_2$ ($w \sim 3$ Hz) and of the OH group ($w \sim 0.8$ Hz) by turning the homonuclear coupling $^3J_{H,O,H} \sim 5$ Hz [43,44] between the ^{13}CH$_2$ and the OH group randomly on and off. This relaxation mechanism is observable in ethanol I but is negligible in ethanol II. For ethanol II the condition $|^2J_{H,C}-^3J_{H,O,C}| < |^3J_{H,O,H}|$ is valid and $^3J_{H,O,H}$ is neither observable nor has an effect on the relaxation process. The width $w_t \sim 0.2$ Hz of the triplet lines in Fig. 8(a) can be explained by a transfer of the fast dephasing process of the ^{13}CH$_2$ group to the protons of the ^{12}CH$_3$ group by the homonuclear $^3J_{H,H}$ coupling: if the ^{13}CH$_2$ group is in the singlet state then this relaxation channel is blocked. Therefore the two intense singlet lines of Fig. 8(a) are narrowed by the suppression of two relaxation channels, the intramolecular dipole-dipole interaction and the relaxation pathway caused by the OH proton exchange.

V. CONCLUSION

We conclude that molecular structures can be investigated by low-field *J*-coupled NMR spectroscopy even in the absence of any chemical shift information. Although at low field, the complexity of the spectra of larger molecules with rare spins in natural abundance is high, we can use the spectral pattern as a fingerprint of the molecular structure. Furthermore, the existence of long-lived singlet states and pairs of singlet states has been proven to exist in various molecules and without the need of special preparation pulse sequences [45,46]. It was shown experimentally that many different transverse relaxation times, which vary by almost two orders of magnitude, exist in small molecules such as ethanol and these relaxation times depend sensitively on the spin state of the molecule. Especially if pairs of spins in the molecule are in a singlet state then different relaxation pathways, such as the dipole-dipole and the *J*-coupling mediated relaxation, are blocked and very narrow lines are observed. From our experiments we are convinced that in future high-resolution NMR experiments will be performed with mobile, low-field spectrometers equipped with magnetically shielded electromagnets, which operate independent of the Earth's magnetic field. Together with hyperpolarization technologies this will allow for investigations of rare spins in natural abundance by mobile NMR. This opens the door for new low-field applications in NMR spectroscopy, magnetic resonance imaging (MRI), quantum computing, and flow and diffusion studies in biology and material science.

[1] R. R. Ernst, G. Bodenhausen, and A. Wokaun, *Principles of Nuclear Magnetic Resonance in One and Two Dimensions* (Clarendon Press, Oxford, UK, 1987).

[2] J. T. Arnold, S. S. Dharmatti, and M. E. Packard, J. Chem. Phys. **19**, 507 (1951).

[3] W. G. Proctor and F. C. Yu, Phys. Rev. **77**, 717 (1950); **81**, 20 (1951).

[4] E. L. Hahn and D. E. Maxwell, Phys. Rev. **88**, 1070 (1952).

[5] J. Kaplan, Phys. Rev. **93**, 939 (1954), see p. 941, M. Packard and R. Varian.

[6] H. Benoit, J. Hennequin, and H. Ottavi, Chimie Analytique **44**, 471 (1962).

[7] B. F. Melton and V. L. Pollak, Rev. Sci. Instrum. **42**, 769 (1971).

[8] G. J. Béné, Phys. Rep. **58**, 213 (1980).

[9] G. J. Béné, B. Borcard, É. Hiltbrand, and P. Magnin, in *NMR in Medicine*, edited by R. Damadian (Springer, Berlin, 1981).

[10] J. Stepišnik, M. Kos, G. Planinšič, and V. Eržen, J. Magn. Reson., Ser. B **107**, 167 (1994).

[11] G. Planinšič, J. Stepišnik, and M. Kos, J. Magn. Reson., Ser. A **110**, 170 (1994).

[12] A. Shushakov, Geophysics **61**, 998 (1996).

[13] P. T. Callaghan, C. D. Eccles, and J. D. Seymour, Rev. Sci. Instrum. **68**, 4263 (1997).

[14] K. Lang, M. Moussavi, and E. Belorizky, J. Phys. Chem. A **101**, 1662 (1997).

[15] P. T. Callaghan, R. Dykstra, C. D. Eccles, T. G. Haskell, and J. D. Seymour, Cold Regions Sci. Technol. **29**, 153 (1999).

[16] R. Goedecke and H. von Boetticher, Z. Med. Phys. **9**, 130 (1999).

[17] R. J. S. Brown, Concepts Magn. Reson. **13**, 344 (2001).

[18] O. R. Mercier, M. W. Hunter, and P. T. Callaghan, Cold Re-

gions Sci. Technol. **42**, 96 (2005).

[19] M. E. Halse *et al.*, J. Magn. Reson. **182**, 75 (2006).

[20] J. N. Robinson *et al.*, J. Magn. Reson. **182**, 343 (2006).

[21] P. J. Hore, J. A. Jones, and S. Wimperis, *NMR: The Toolkit* (Oxford University Press, Oxford, 2000).

[22] M. Burghoff, S. Hartwig, L. Trahms, and J. Bernarding, Appl. Phys. Lett. **87**, 054103 (2005).

[23] M. A. Bouchiat, T. R. Carver, and C. M. Varnum, Phys. Rev. Lett. **5**, 373 (1960).

[24] F. D. Colegrove, L. D. Schearer, and G. K. Walters, Phys. Rev. **132**, 2561 (1963).

[25] W. Happer, Rev. Mod. Phys. **44**, 169 (1972).

[26] B. Driehuys *et al.*, Appl. Phys. Lett. **69**, 1668 (1996).

[27] S. Appelt *et al.*, Phys. Rev. A **58**, 1412 (1998).

[28] C. R. Bowers and D. P. Weitekamp, Phys. Rev. Lett. **57**, 2645 (1986).

[29] M. Goldman, H. Jóhannesson, O. Axelsson, and M. Karlsson, Magn. Reson. Imaging **23**, 153 (2005).

[30] G. Navon *et al.*, Science **271**, 1848 (1996).

[31] S. Appelt, F. W. Häsing, S. Baer-Lang, N. J. Shah, and B. Blümich, Chem. Phys. Lett. **348**, 263 (2001).

[32] Y. S. Greenberg, Rev. Mod. Phys. **70**, 175 (1998).

[33] R. McDermott *et al.*, Science **295**, 2247 (2002).

[34] A. H. Trabesinger *et al.*, J. Phys. Chem. A **108**, 957 (2004).

[35] J. Bernarding *et al.*, J. Am. Chem. Soc. **128**, 714 (2006).

[36] I. K. Kominis, T. W. Kornack, J. C. Allred, and M. V. Romalis, Nature (London) **422**, 596 (2003).

[37] I. M. Savukov and M. V. Romalis, Phys. Rev. Lett. **94**, 123001 (2005).

[38] I. M. Savukov, S.-K. Lee, and M. V. Romalis, Nature (London) **442**, 1021 (2006).

[39] C. A. Meriles, D. Sakellariou, D. H. Heise, A. J. Moulé, and A. Pines, Science **293**, 82 (2001).

[40] J. Perlo *et al.*, Science **308**, 1279 (2005).

[41] S. Appelt, F. W. Häsing, H. Kühn, J. Perlo, and B. Blümich, Phys. Rev. Lett. **94**, 197602 (2005).

[42] S. Appelt, H. Kühn, F. W. Häsing, and B. Blümich, Nat. Phys. **2**, 105 (2006).

[43] S. Appelt, F. W. Häsing, H. Kühn, U. Sieling, and B. Blümich, Chem. Phys. Lett. **440**, 308 (2007).

[44] F. A. Bovey, *NMR Data Tables for Organic Compounds* (Wiley Interscience, New York, 1967).

[45] M. Carravetta, O. G. Johannessen, and M. H. Levitt, Phys. Rev. Lett. **92**, 153003 (2004).

[46] M. Carravetta and M. H. Levitt, J. Chem. Phys. **122**, 214505 (2005).

[47] B. W. Koenig and K. Gawrisch, J. Phys. Chem. B **109**, 7540 (2005).